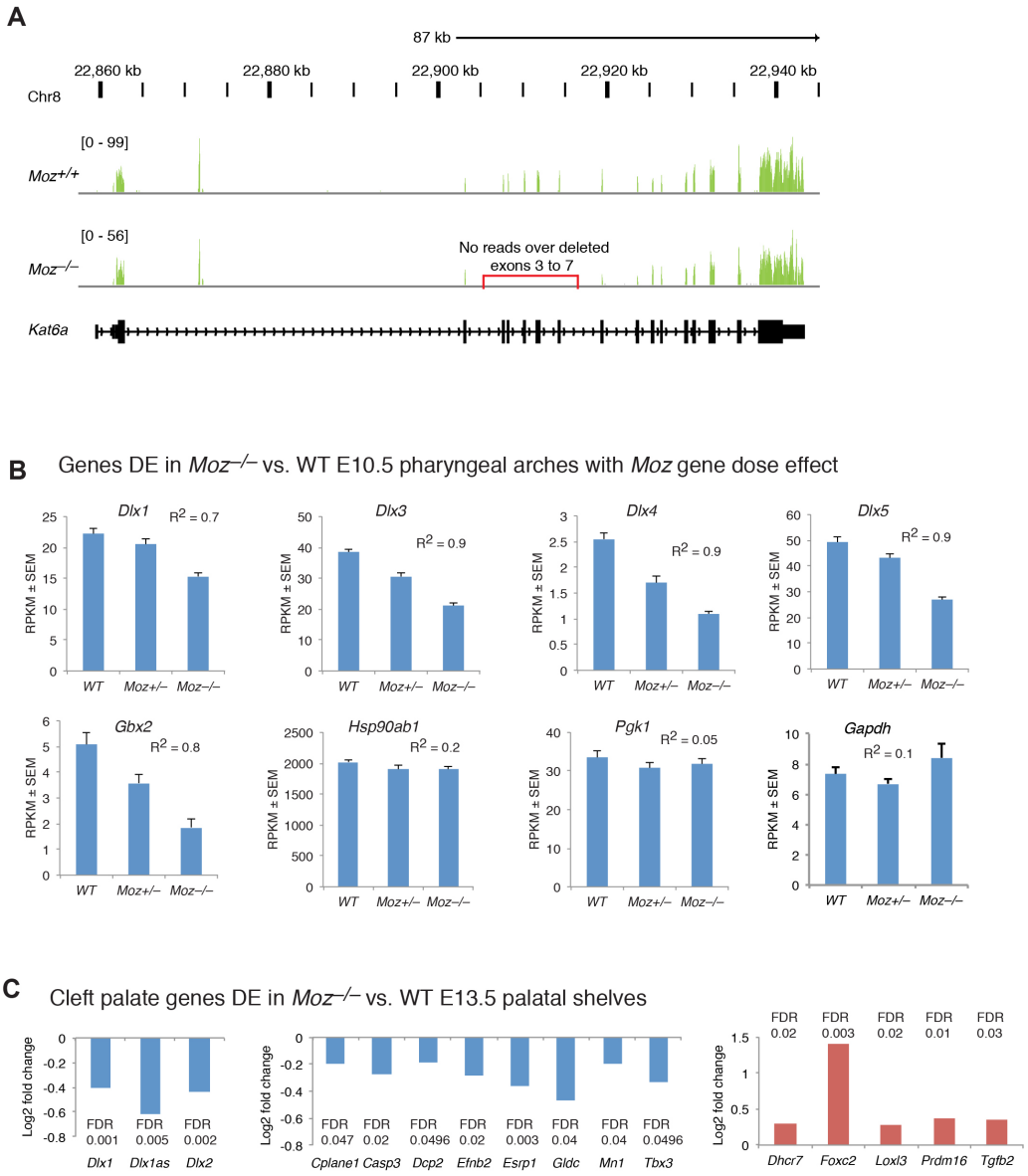

Fig. S1. MOZ gene dosage effects on *Dlx* gene expression in E10.5 1st and 2nd pharyngeal arches and differential gene expression in E13.5 *Moz*$^{-/-}$ vs. wild type palatal shelves.

(A) RNA-seq coverage plots for the *Moz* gene. Results are shown for one of the four animals of each genotype. *Moz*$^{-/-}$ animals lack exons 3 to 7 of the locus and so lack reads in this region.

(B) mRNA levels as reads per kilobase per million reads (RPKM) of *Dlx* genes and *Gbx2* that show a *Moz* gene dosage effect compared to the house keeping genes *Hsp90ab1, Pgk1* and *Gapdh.* The entire list of genes differentially expressed between E10.5 *Moz*$^{-/-}$ and *Moz*$^{+/+}$ 1st and 2nd pharyngeal arches is provided, with p values and FDRs, in **Table S1** (Excel file).

(C) Log_2-fold change in mRNA levels between E13.5 *Moz*$^{-/-}$ and *Moz*$^{+/+}$ palatal shelves of *Dlx1* and *Dlx2*, as well as other genes associated with cleft palate. The entire list of genes differentially expressed between E13.5 *Moz*$^{-/-}$ and *Moz*$^{+/+}$ palatal shelves is provided, with p values and FDRs, in **Table S2**.

N = 4 E10.5 embryos for each genotype. Data were analysed as described under RNA-seq analysis.

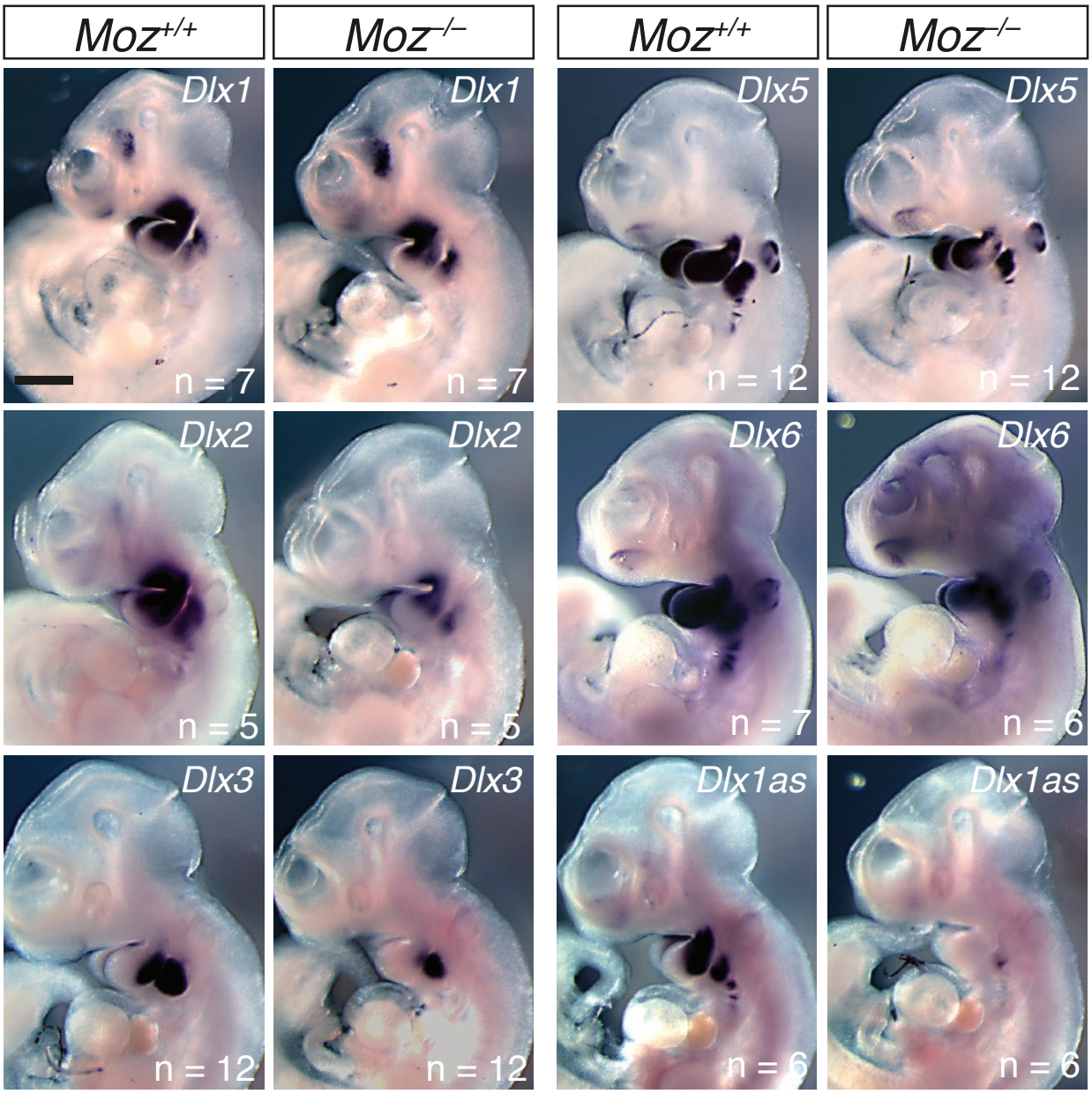

Fig. S2. Expression domains of *Dlx* genes in *Moz*$^{-/-}$ embryos are reduced in size.

Whole mount *in situ* hybridisation of E10.5 *Moz*$^{+/+}$ and *Moz*$^{-/-}$ embryos detecting *Dlx* family gene mRNA (dark purple stain). *Endpoint-staining* to reveal changes in the expression domains of the *Dlx* family genes in *Moz*$^{-/-}$ compared to wild type controls. Embryos are representative of each experiment. N = as indicated. Scale bar = 550 μm.

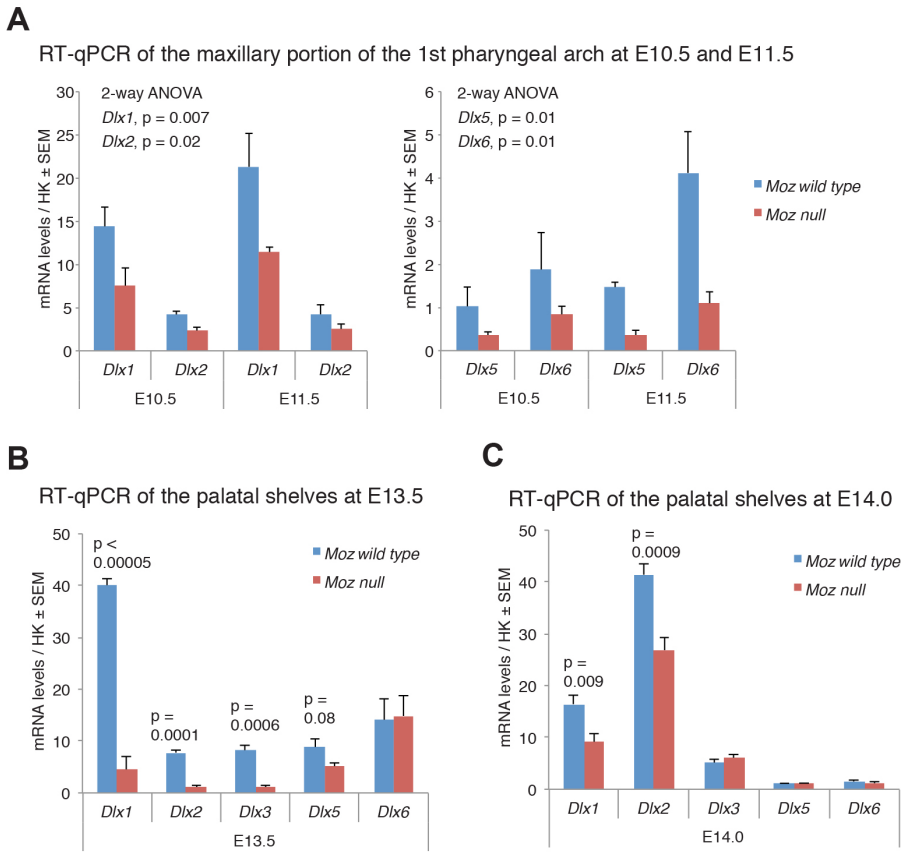

Fig. S3. Loss of MOZ affects *Dlx* family gene expression throughout palate development.

RT-qPCR assessment of *Dlx* gene family mRNA levels in *Moz*$^{-/-}$ vs. wild type isolated maxillary component of the 1st pharyngeal arch at E10.5 and E11.5, as well as in *Moz*$^{-/-}$ vs. wild type isolated palatal shelves at E13.5 and E14.5.

N = 4 embryos per developmental stage and genotype. Data are displayed as mean ± s.e.m. and were analysed by two-way ANOVA with *Moz* genotype and developmental stage as the two independent factors (A) or by one-way ANOVA (B,C).

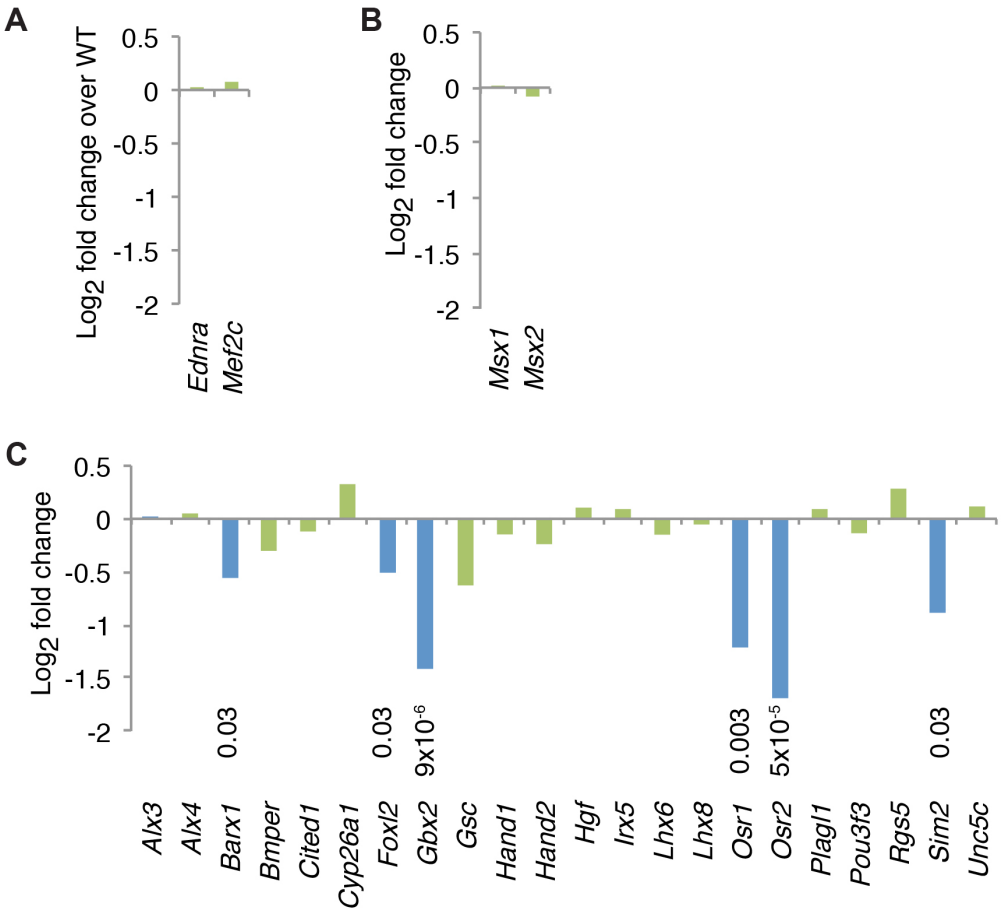

Fig. S4. Quantitative assessment of changes in expression of DLX transcription factor target genes in *Moz*$^{-/-}$ vs. wild type 1st and 2nd pharyngeal arches.

(A) mRNA levels of genes that encode upstream regulators of *Dlx* family genes are unchanged in E10.5 *Moz*$^{-/-}$ vs. wild type 1st and 2nd pharyngeal arches, note log_2-fold change in mRNA levels is not statistically different from 0.

(B) mRNA levels of genes that encode proteins that operate at the same level as DLX proteins are unchanged in E10.5 *Moz*$^{-/-}$ vs. wild type 1st and 2nd pharyngeal arches, note log_2-fold change in mRNA levels is not statistically different from 0.

(C) Log_2-fold change in mRNA levels of genes that encode downstream target genes of DLX family transcription factors differentially expressed in E10.5 *Moz*$^{-/-}$ vs. wild type 1st and 2nd pharyngeal arches.

P values and FDRs are provided in **Table S1**.

N = 4 E10.5 embryos for each genotype. Data were analysed as described under RNA-seq analysis.

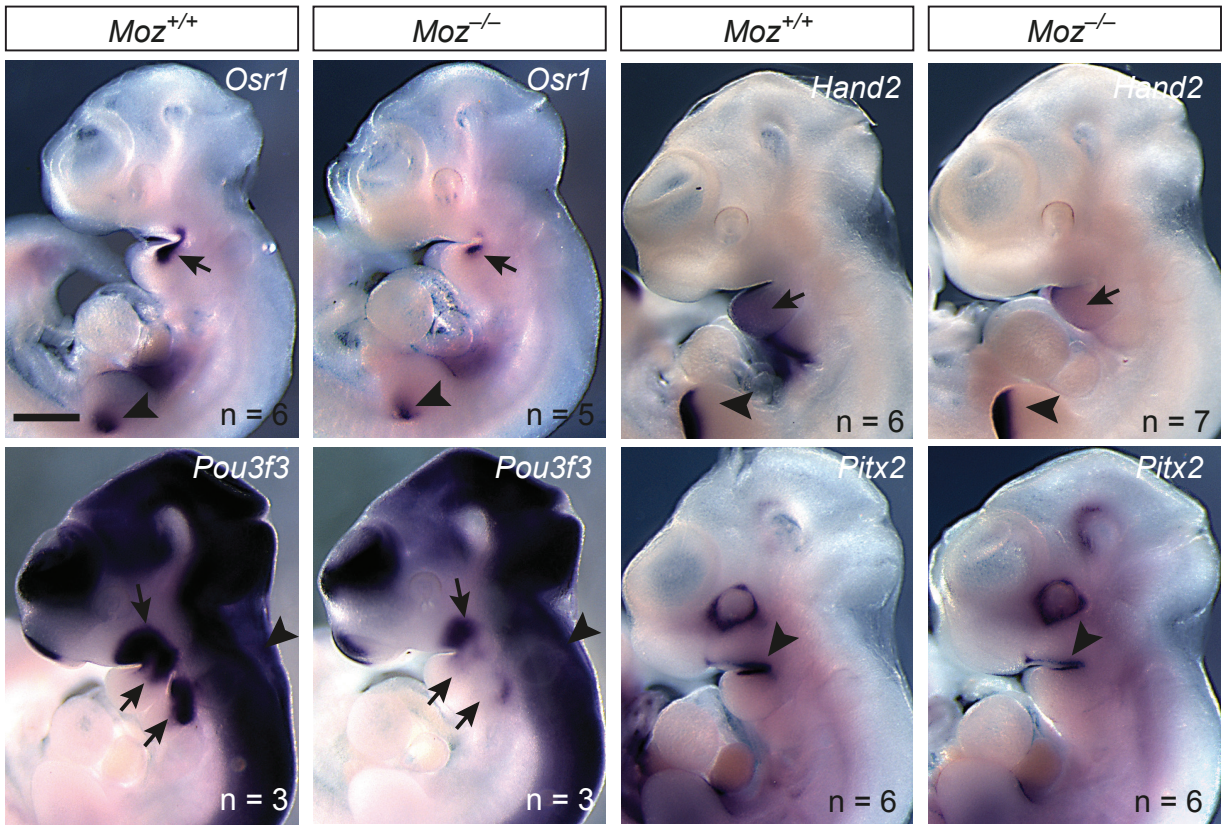

Fig. S5. Genes downstream of DLX transcription factors are affected by loss of MOZ.

Whole mount *in situ* hybridisation on E10.5 *Moz*$^{+/+}$ and *Moz*$^{-/-}$ embryos probed for genes downstream of DLX transcription factors *(Osr1, Pou3f3, Hand2)* and upstream of *Dlx* gene expression *(Pitx2)*. Arrows indicate pharyngeal arch expression domains that are affected by the loss of MOZ. Arrowheads indicate expression domains outside the pharyngeal arches (*Osr1*, *Hand2*, *Pou3f3*) or the unaffected pharyngeal arch domain of *Pitx2*. Embryos are representative of each experiment. Endpoint staining. N, number of embryos as indicated. Scale bar = 550 µm.

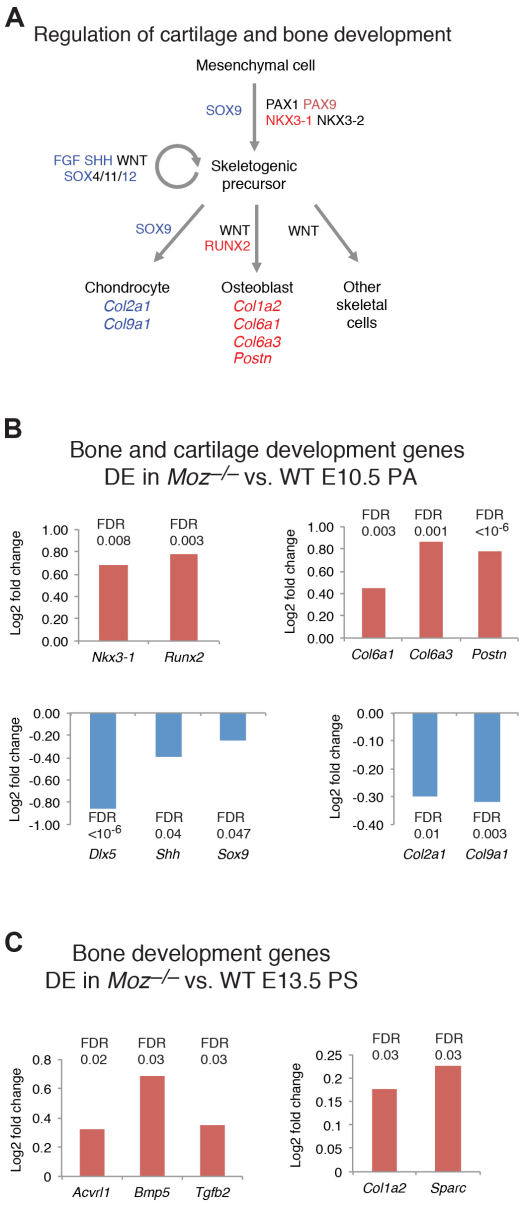

Fig. S6. MOZ affects the expression of genes encoding regulators and effectors of bone development.

(A) Schematic drawing of the skeletogenic cell lineage based on publications reviewed in (Hartmann, 2009; Lefebvre and Bhattaram, 2010). Genes upregulated in *Moz*$^{-/-}$ vs. wild type are indicated in red font, downregulated in blue font. One member of the WNT family that has been shown to increase palatal mesenchymal cell proliferation is WNT6 (Jiang et al., 2017).

(B) Log_2-fold change in mRNA levels of genes differentially expressed in E10.5 *Moz*$^{-/-}$ vs. wild type 1st and 2nd pharyngeal arches.

(C) Log_2-fold change in mRNA levels of genes differentially expressed in E13.5 *Moz*$^{-/-}$ vs. wild type palatal shelves.

P values and FDRs are provided in **Tables S1,S2.**

N = 4 embryos per genotype and developmental stage. Data were analysed as described under RNA-seq analysis.

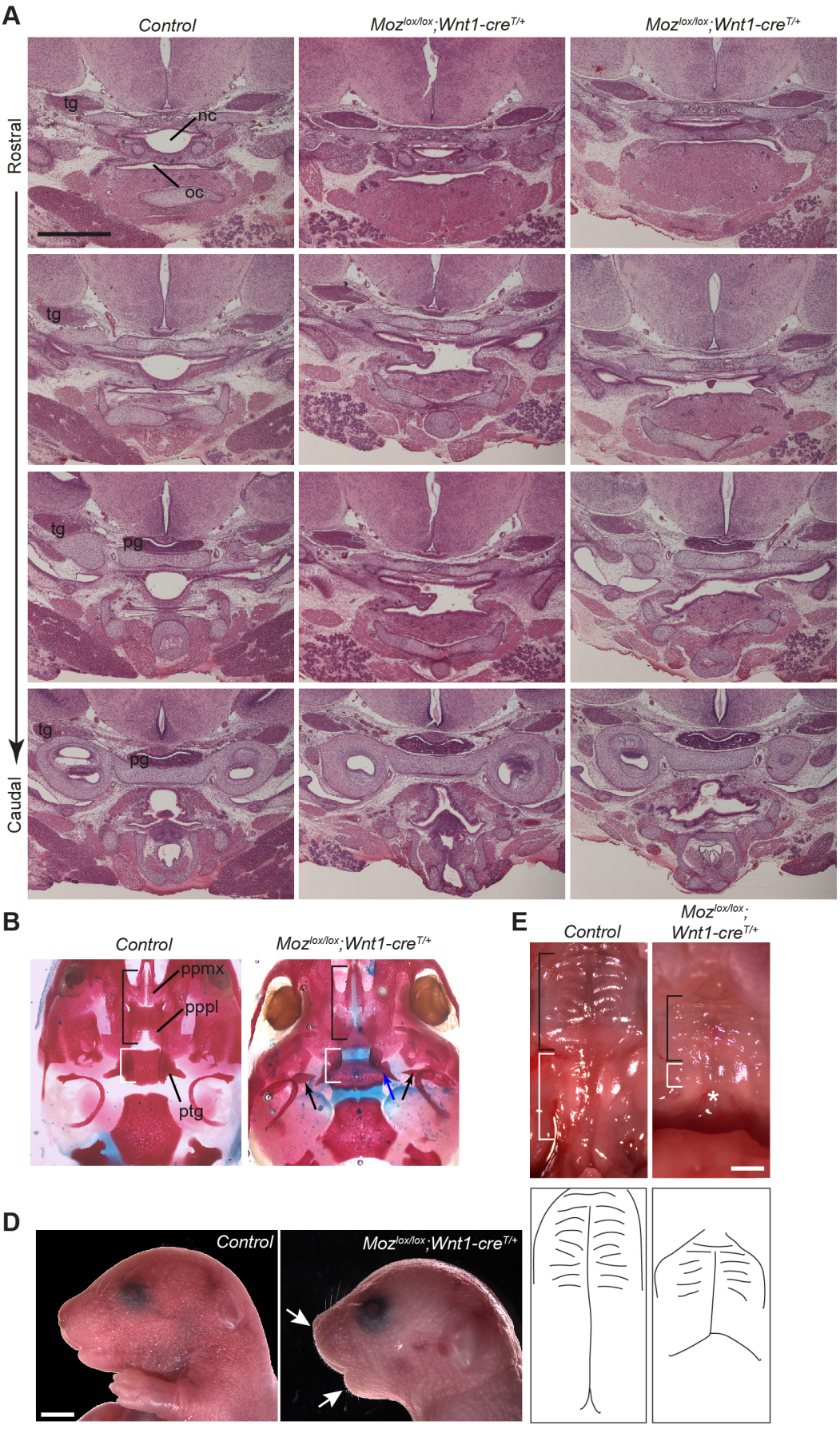

Fig. S7. Serial sections, skeletal preparations and gross morphology of *Moz$^{lox/lox}$;Wnt1-cre$^{T/+}$* mice.

(A) Serial frontal H&E stained sections of the E18.5 heads of two *Moz$^{lox/lox}$;Wnt1-cre$^{T/+}$* pups and

one control pup at four rostro-caudal levels spanning the anatomical location of the soft palate from the most rostral level that still displayed an intact palate in the *Moz*$^{lox/lox}$*;Wnt1-cre*$^{T/+}$ pups to the first section displaying parts of the pharynx. Note the disrupted barrier between the oral cavity (oc) and the nasal cavity (nc). The physical distance between the levels was comparable between controls and *Moz*$^{lox/lox}$*;Wnt1-cre*$^{T/+}$ pups. The trigeminal ganglion (tg) and the pituitary gland (pt) are indicated as landmarks.

(B) Ventral view of the skull, lower jaw removed. Note the relatively normal ratios of the structure contributing to the hard palate (black brackets) vs. the anatomical location of the soft palate (white brackets). The extents of palatine processed of the palatine (pppl) and the maxillary bone (ppmx) appear similar in the *Moz*$^{lox/lox}$*;Wnt1-cre*$^{T/+}$ and the control. In contrast, the pterygoid bone (ptg) is malformed in the *Moz*$^{lox/lox}$*;Wnt1-cre*$^{T/+}$ skull (blue arrow). Note the abnormal additional bone (black arrows), which, like the os paradoxicum in *Dlx5*$^{-/-}$ skulls, is positioned caudal of alisphenoid bone [compare to Fig. 6T,6T'].

(D) External appearance of the head at birth. Most *Moz*$^{lox/lox}$*;Wnt1-cre*$^{T/+}$ pups had a normal external appearance, including apparently normal jaws. One atypical *Moz*$^{lox/lox}$*;Wnt1-cre*$^{T/+}$ pup showed shortening of the upper and lower jaw. This most severely affected *Moz*$^{lox/lox}$*;Wnt1-cre*$^{T/+}$ pup is displayed here. Arrows indicate shortened upper and lower jaw.

(E) Top two panels: ventral view of the palate of the pups shown in (D). Black bracket indicates region of the hard palate, white bracket region of the soft palate, asterisks cleft of the soft palate. Right two panels: line drawing of left panels to indicate structural differences

N = 6 animals per genotype examined. Scale bars equal 1 mm (A), 860 µm (B), 2 mm (D) and 1 mm (E)

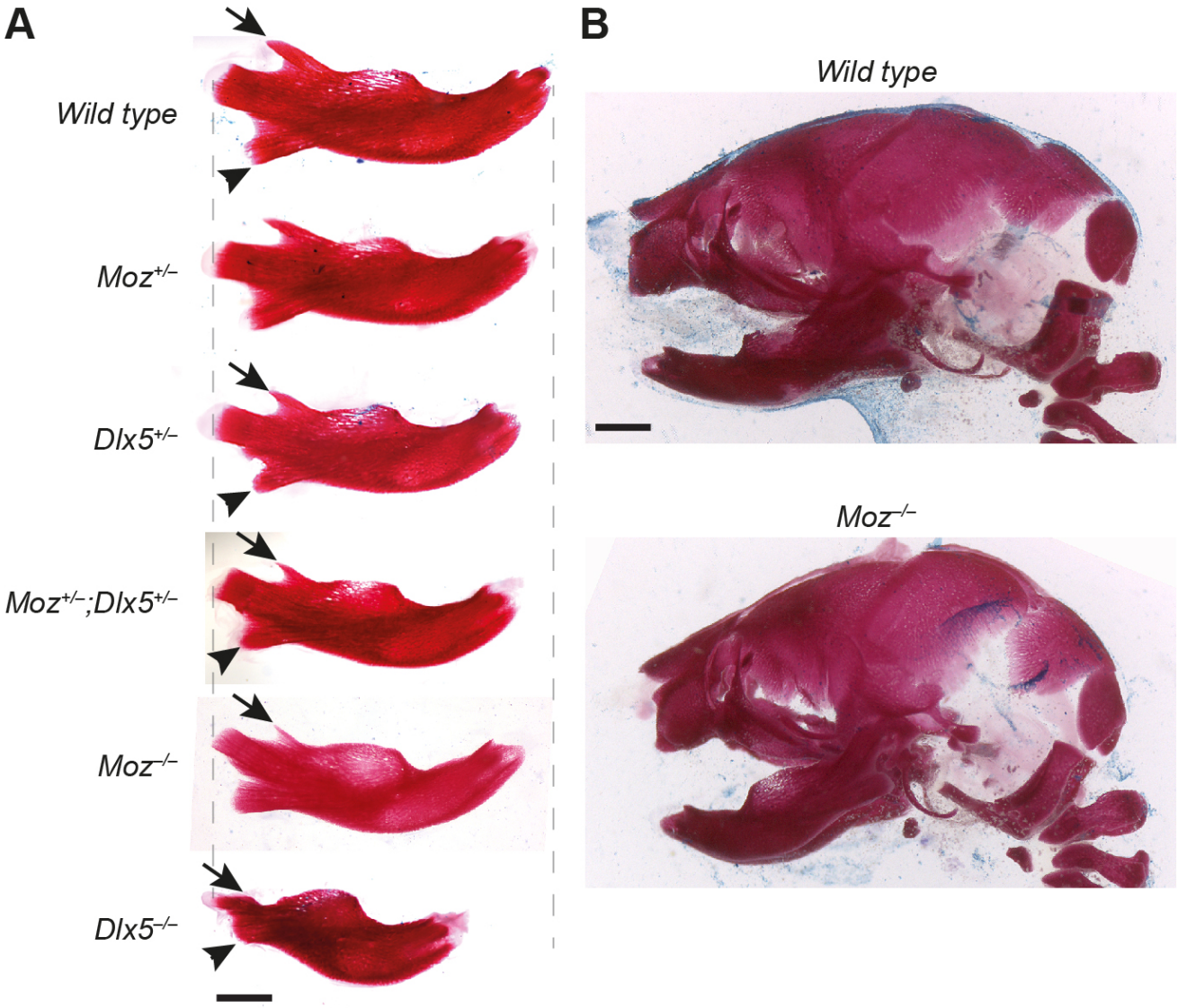

Fig. S8. *Moz;Dlx5* double heterozygous animals have a shortened lower jaw.

(A) Alizarin red staining of the lower jaw bone of E18.5 wild type, single *Moz* or *Dlx5* heterozygotes, *Moz;Dlx5* double heterozygotes, *Moz* homozygous and *Dlx5* homozygous mutant foetuses revealed progressively shorter jaw in the single heterozygotes, double heterozygotes and homozygote animals compared to wild type controls. The coronoid process (arrow) was also progressively reduced. In contrast, the angular process (arrowhead) appeared to be more influenced by the loss of one or two alleles of *Dlx5* than by loss of *Moz* alleles. Scale bar = 820 μm.

(B) Lateral view of E18.5 wild type and *Moz* homozygous skulls with lower jaw attached. Scale bar = 640 μm.

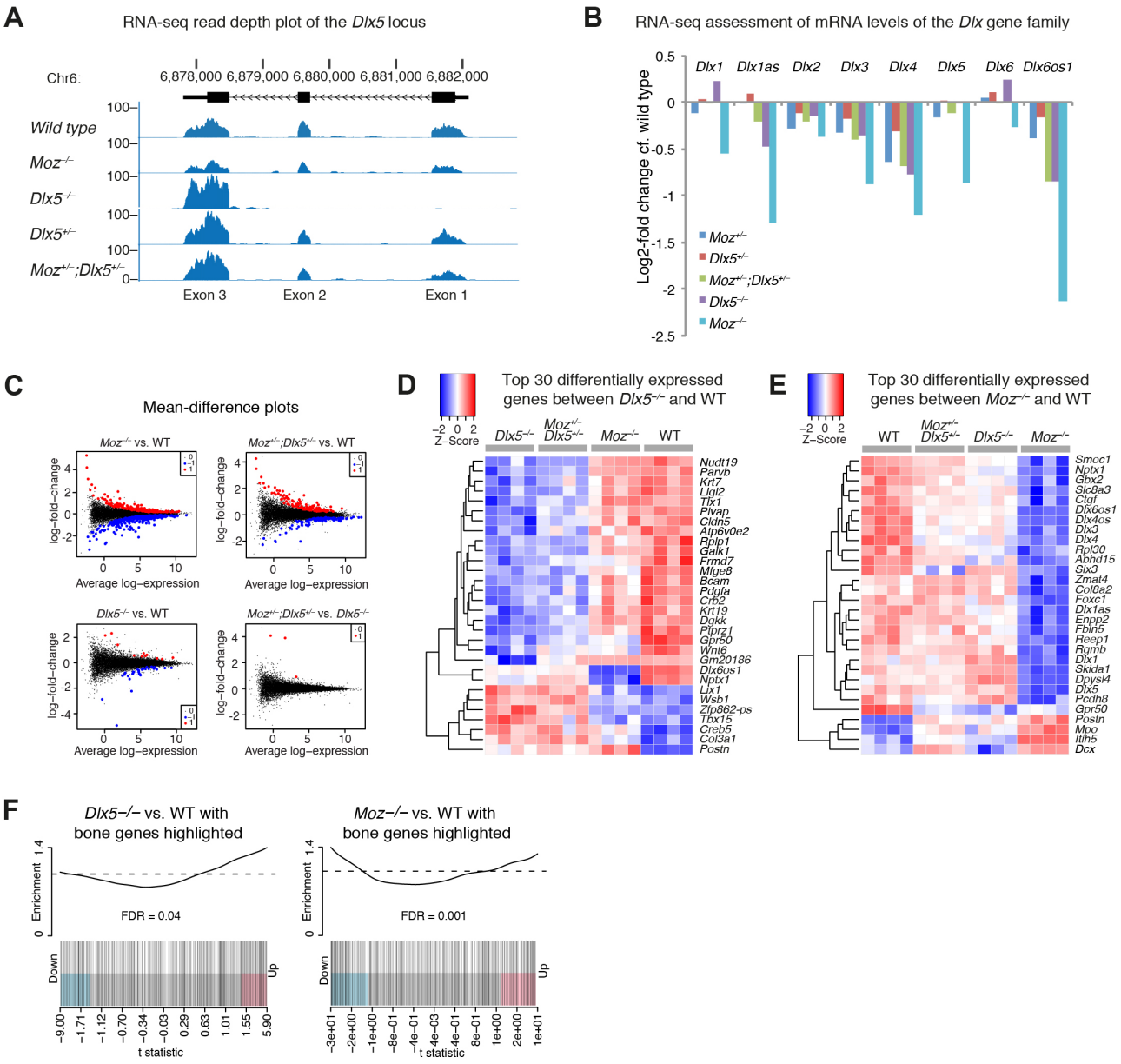

Fig. S9. *Moz;Dlx5* mutant pharyngeal arch transcriptome analysis.

RNA sequencing experiments comparing E10.5 1st and 2nd pharyngeal arches of wild type, *Moz*$^{+/-}$, *Dlx5*$^{+/-}$, *Moz*$^{+/-}$;*Dlx5*$^{+/-}$ double heterozygotes, *Dlx5*$^{-/-}$ and *Moz*$^{-/-}$ embryos.

(A) RNA-seq coverage plots for the *Dlx5* gene. Results are shown for one of the four animals for each genotype. *Dlx5*$^{-/-}$ animals lack exons 1 and 2 of the locus, but have increased reads in exon 3 when compared to wild type. *Moz*$^{-/-}$ have a reduced number of reads on all *Dlx5* exons compared to wild type, and *Moz*$^{+/-}$;*Dlx5*$^{+/-}$ double heterozygotes display levels intermediate between *Moz*$^{-/-}$ and wild type samples in exons 1 and 2.

(B) Log_2 fold changes in *Dlx* family gene expression in each genotype relative to wild type controls. Positive log fold changes show upregulation in the mutant; negative values indicate downregulation. FDRs are displayed in **Table S3**.

(C) Mean difference plots reveal many genes differentially expressed between *Moz*$^{-/-}$ and wild type pharyngeal arches and few differences between *Dlx5*$^{-/-}$ and wild type samples. Although *Moz*$^{+/-}$*;Dlx5*$^{+/-}$ double heterozygotes display many differences to wild type, they are similar to *Dlx5*$^{-/-}$ pharyngeal arches. Y-axes show $\log_2$ fold changes in expression levels. X-axis shows average $\log_2$-expression ($\log_2$ counts per million).

(D) Heatmap of the top 30 genes differentially expressed between *Dlx5*$^{-/-}$ and wild type pharyngeal arches. Genes are grouped by hierarchical clustering. Similar to **Figure 7E**, this comparison indicates similarities between the *Moz*$^{+/-}$*;Dlx5*$^{+/-}$ double heterozygotes and *Dlx5*$^{-/-}$ samples.

(E) Heatmap of the top 30 genes differentially expressed between *Moz*$^{-/-}$ and wild type pharyngeal arches. Genes are grouped by hierarchical clustering and show that, while *Moz*$^{-/-}$ samples are dissimilar to other the genotypes, many gene expression changes in the *Moz* and *Dlx5* genotypes have the same direction.

(F) Barcode plots showing up or down regulation of bone development genes in various genotypes relative to wild type. *Moz*$^{-/-}$ display a mixed response for bone genes, whereas bone genes are enriched among the genes upregulated in *Dlx5*$^{-/-}$ compared to wild type, as they are in *Moz*$^{+/-}$*;Dlx5*$^{+/-}$ compared with wild type (see **Figure 7H**).

All data shown are from N = 4 female E10.5 embryos for each of the 6 genotypes.

Table S1 supplied in Excel file displays RNA-seq results of genes differentially expressed in E10.5 *Moz*$^{-/-}$ vs. wild type 1st and 2nd pharyngeal arches.

Table S2 supplied in Excel file displays RNA-seq results of genes differentially expressed in E13.5 *Moz*$^{-/-}$ vs. wild type palatal shelves.

Table S3 supplied in Excel file displays the comparison of craniofacial skeletal anomalies between genotypes *Moz*$^{lox/lox}$*;Wnt1-cre*$^{T/+}$, *Moz*$^{+/-}$ single heterozygotes, *Dlx5*$^{+/-}$ single heterozygotes, *Moz*$^{+/-}$*;Dlx5*$^{+/-}$ compound heterozygotes, *Dlx5*$^{-/-}$ single knockout and *Moz*$^{-/-}$ single knockout mouse data from this study and data from the literature on *Dlx1*$^{+/-}$*;Dlx2*$^{+/-}$*;Dlx3*$^{+/-}$*;Dlx5*$^{+/-}$*;Dlx6*$^{+/-}$ compound heterozygotes, *Dlx5*$^{-/-}$ single knockout, *Dlx2*$^{-/-}$ single knockout and *Dlx1*$^{-/-}$ single knockout mice.

Click here to Download Tables S1 - S3

Table S4: FDRs for difference between *Moz* and/or *Dlx5* mutants vs. wild-type controls (WT) for selected differentially expressed genes

Gene	Direction of change	All *Moz* and *Dlx5* genotypes vs. WT*	Cleft palate genotypes vs. WT*	$Moz^{-/-}$ vs. WT	$Dlx5^{-/-}$ vs. WT
Upstream regulators of *Dlx* genes					
Ednra	↑	0.047	0.09	1	0.1
Fgf8	±0	0.06	0.06	0.2	0.2
Pitx2	±0	0.6	0.7	0.8	0.4
Mef2c	±0	0.5	0.5	0.7	0.7
Dlx gene family					
Dlx1	↓	0.5	0.4	$8x10^{-6}$	0.4
Dlx1as	↓	0.04	0.002	$6x10^{-8}$	0.2
Dlx2	↓	0.1	0.2	0.02	0.7
Dlx3	↓	0.0004	$4x10^{-5}$	$2x10^{-9}$	0.1
Dlx4	↓	0.003	0.0008	$8x10^{-6}$	0.1
Dlx5	↓	0.04	0.008	$2x10^{-9}$	1
Dlx6	±0	0.9	1	0.07	0.5
Dlx6os1	↓	$4x10^{-10}$	$3x10^{-13}$	$9x10^{-18}$	$3x10^{-5}$
Confirmed direct target of DLX transcription factors					
Gbx2	↓	0.03	0.008	$9x10^{-6}$	0.3
Inducers of self-renewal of bipotential skeletogenic precursors					
Shh	↓	0.08	0.05	0.04	0.2
Wnt6	↓	0.01	0.008	0.02	0.02
Bone development inducing genes					
Pax9	↑	0.009	0.009	0.1	0.2
Runx2	↑	0.0004	0.0008	0.003	0.06
Genes encoding proteinaceous extracellular matrix					
Col1a2	↑	0.02	0.01	0.7	0.05
Col6a3	↑	0.02	0.01	0.04	0.2
Postn	↑	$6x10^{-5}$	$4x10^{-6}$	$2x10^{-8}$	0.01

* All *Moz and Dlx5* genotypes: $Moz^{+/-}$, $Dlx5^{+/-}$, $Moz^{+/-}$;$Dlx5^{+/-}$, $Moz^{-/-}$, $Dlx5^{-/-}$ *vs. WT*
Cleft palate genotypes: $Moz^{+/-}$;$Dlx5^{+/-}$, $Moz^{-/-}$, $Dlx5^{-/-}$.

DLX target genes are based on (Barron et al., 2011; Jeong et al., 2008). Upstream regulators of *Dlx* genes are based on (Charite et al., 2001; Green et al., 2001; Thomas et al., 2000; Verzi et al., 2007). Skeletogenic cell lineage are based on publications reviewed in (Hartmann, 2009; Lefebvre and Bhattaram, 2010).

Table S5 supplied in Excel file displays RNA-seq results of genes differentially expressed in the 1st and 2nd pharyngeal arches of E10.5 wild type, $Moz^{+/-}$, $Dlx5^{+/-}$, $Moz^{+/-}$;$Dlx5^{+/-}$ double heterozygotes, $Dlx5^{-/-}$ and $Moz^{-/-}$ embryos.

Click here to Download Table S5

Table S6: Whole mount in situ hybridisation sense and antisense probe templates

Target gene	Generated by primer sequences (5' to 3')	Length	Accession number
Dlx1	Fwd: TCGGGCTGAAAGGTCGCTGAGTC Rev: CACCCAGACCCCGCGAGAAGAGAT	1029 bp	NCBI: NM_010053.2|
Dlx2	IMAGE clone obtained from RZPD	2192 bp	GenBank: BC094317.1
Dlx3	Fwd: GGCCACCGATTCTGACTACTA Rev: CATCAGGGGGCAGAAGAAAGTTAGC	1307 bp	NCBI: NM_010055
Dlx5	Fwd: GGCCACCGATTCTGACTACTA Rev: AAAAAGGGGGCGGGGCTCTC	931 bp	NCBI: NM_010056.3
Dlx6	Fwd: CCCCCAAAGTTTTGATGATG Rev: AGAAACGTCCCACACTGGAG	799 bp	UCSC: uc009aww.1
Dlx1as	Fwd: GAAGACCTCATGCAGCACAA Rev: GACCTTCGCAGTCTTTCAGG	1145 bp	RefSeq: NR_002854.2
Pitx2		900 bp	NCBI: NM_011098
Gsc	Fwd: GCATGTTCAGCATCGACAAC Rev: CAGTCCTGGGCCTGTACATT	909 bp	UCSC: uc007oxh.1
Gbx2	Fwd: GAGTCAAAGGTGGAAGATGACC Rev: CAAACGAGCAGAGCAGAGTTC	995 bp	UCSC: uc007bzb.1
Hand2	Fwd: CGAGGAGAACCCCTACTTCC Rev: GATAACCGACCCGACAGAAA	1039 bp	UCSC: uc009lss.2
Sim2	Fwd: TGCAGCGGCTACCTAAAGAT Rev: GCTGGGCACTAGAGAGTTGG	948 bp	UCSC: uc008aae.1
Osr1	Fwd: GCTGTCCACAAGACGCTACA Rev: TCAGCATAAAGTGCCAGTCG	856 bp	UCSC: ux007nao.2
Osr2	Fwd: TCTTTACACATCCCGCTTCC Rev: TCCTTTCCCACACTCCTGAC	1023 bp	UCSC: uc007vma.1
Pou3f3	Fwd: CAGCCTACAGCTGGAAAAGG Rev: TTTACTGCGGAGGATGCTTT	1084 bp	UCSC: uc007auw.1

Table S7: Oligonucleotide primers for RT-qPCR and for ChIP-qPCR

RT-qPCR primers

Target Gene	Primer sequences (5' to 3')	Description of amplicon	Accession number
Dlx1	Fwd: TCCAGCCCCTACATCAGTTC Rev: TCTTTTTCCCTTTGCCGTTA	Exons 2-3	UCSC: uc008kau.1
Dlx2	Fwd: CTTCTGCATCCTTCGCAGAC Rev: CAAGTCTCAGACGCTGTCCA	Exons 4-5	UCSC: uc008kax.2
Dlx3	Fwd: TAACCCTGGGGCTGTGTACT Rev: CTAGGACAGGGCACCTTCTG	Exons 4-5	UCSC: uc007kzy.2
Dlx4	Fwd: GTCTACCCAAGGCAGACACC Rev: TGACAGGAGGGCTGAAGTCT	Within exon 3	UCSC: uc007kzz.2
Dlx5	Fwd: AGCCCCTACCACCAGTACG Rev: CAGGGCGAGGTACTGAGTCT	Exons 1-2	UCSC: uc009awz.1
Dlx6	Fwd: ATTCCTCACCACACCAGGAC Rev: CTGCCATGTTTGTGCAGATT	Exons 4-6	UCSC: uc009aww.1
Dlx1as	Fwd: GCCTTCGACCCTTTTGATTT Rev: TCCTGGACCACTTTTTCCTG	Exons 1-2	RefSeq: NR_002854.2
Dlx6os1	Fwd: AGGGAACGGGGATATTGAAC Rev: ACTCCACAGCAGTGGGAAAG	Exons 1-2	UCSC: uc009awu.1
Hsp90ab1	Fwd: AGAATCCGACACCAAACTGC Rev: ACCTGGGAACCATTGCTAAG	Exon 10	NCBI: NM_008302
Pgk1	Fwd: TACCTGCTGGCTGGATGG Rev: CACAGCCTCGGCATATTTCT	Exons 8-9	NCBI: NM_008828
Gapdh	Fwd: TTCACCACCATGGAGAAGGC Rev: CCCTTTTGGCTCCACCCT	Exons 3-4	NCBI: NM_001289726.1
Psmb2	Fwd: GAGGGCAGTGGAGCTTCTTA Rev: AGGTGGGCAGATTCAAGATG	Exons 5-6	NCBI: NM_011970.4
Rpl13a	Fwd: GGAGAAACGGAAGGAAAAGG Rev: TGAGGACCTCTGTGAACTTGC	Exons 7-8	NCBI: NM_009438

*Primers were designed to be intron-spanning and towards the 3' end (close to the poly-A site) where possible.

ChIP-qPCR primers

Name of primer set	Primer sequences (5' to 3')	Location relative to TSS or chr. position	Description of amplicon position
Hsp90ab1	Fwd: AATTGACATCATCCCCAACC Rev: TCGTGCCAGACTTAGCAATG	+360 bp	Within *Hsp90ab1* exon 3
Dlx5_5'	Fwd: TGACAGAGGCTTGGAGTCCT Rev: TCCTCTTCTGGTTCCCCTTT	-1447 bp	Within intergenic region (IR), 5' of *Dlx5* promoter
Dlx5_1	Fwd: AGGTTTAATCGGGTGTTTTGC Rev: CCAAATCCCTTAGCCTCTTTG	+732 bp	Between *Dlx5* exons 1 & 2
Dlx5_2	FWD: ACCTCTGAGTGTCCCGGTAA REV: CCCCGTTTTTCATGATCTTC	+3536 bp	Overlap 5' intron-exon boundary of *Dlx5* exon 3
ei enhancer	FWD: GTCAGAGCCCAAACCTTGAA REV: TCTCCTCTCAGACTCTCCAAGC	+0 bp (*Dlx6os1*)	Within ei enhancer sequence - overlaps TSS of *Dlx6os1*
Dlx5_11	Fwd: CAATTGAAGCCAGATGGGCG Rev: ATCCGCTGTTGGGAATTGGT	chr6: 6888470-6888600	Peak detected by ChIP-seq in *Dlx5/6 locus* and confirmed by ChIP-qPCR, see Figure 3
Dlx5_12	Fwd: TAGCCTTGTGCGTTTGGACT Rev: GGCAGCTCTCCACTGTCTTT	chr6:6833400-6834000	Peak detected by ChIP-seq in Dlx5/6 locus and confirmed by ChIP-qPCR, see Figure 3
Dlx5_13	Fwd: GAGGAGGCCAGAAGAGGGTA Rev: AGAGGACCTGGGGTGGATTC	chr6: 6800200-6801000	Peak detected by ChIP-seq in *Dlx5/6 locus* and confirmed by ChIP-qPCR, see Figure 3

TSS, transcription start site.

References

Barron, F., Woods, C., Kuhn, K., Bishop, J., Howard, M. J. and Clouthier, D. E. (2011). Downregulation of Dlx5 and Dlx6 expression by Hand2 is essential for initiation of tongue morphogenesis. *Development* **138**, 2249-2259.

Charite, J., McFadden, D. G., Merlo, G., Levi, G., Clouthier, D. E., Yanagisawa, M., Richardson, J. A. and Olson, E. N. (2001). Role of Dlx6 in regulation of an endothelin-1-dependent, dHAND branchial arch enhancer. *Genes Dev* **15**, 3039-3049.

Green, P. D., Hjalt, T. A., Kirk, D. E., Sutherland, L. B., Thomas, B. L., Sharpe, P. T., Snead, M. L., Murray, J. C., Russo, A. F. and Amendt, B. A. (2001). Antagonistic regulation of Dlx2 expression by PITX2 and Msx2: implications for tooth development. *Gene Expr* **9**, 265-281.

Hartmann, C. (2009). Transcriptional networks controlling skeletal development. *Curr Opin Genet Dev* **19**, 437-443.

Jeong, J., Li, X., McEvilly, R. J., Rosenfeld, M. G., Lufkin, T. and Rubenstein, J. L. (2008). Dlx genes pattern mammalian jaw primordium by regulating both lower jaw-specific and upper jaw-specific genetic programs. *Development* **135**, 2905-2916.

Jiang, Z., Pan, L., Chen, X., Chen, Z. and Xu, D. (2017). Wnt6 influences the viability of mouse embryonic palatal mesenchymal cells via the beta-catenin pathway. *Exp Ther Med* **14**, 5339-5344.

Lefebvre, V. and Bhattaram, P. (2010). Vertebrate skeletogenesis. *Curr Top Dev Biol* **90**, 291-317.

Thomas, B. L., Liu, J. K., Rubenstein, J. L. and Sharpe, P. T. (2000). Independent regulation of Dlx2 expression in the epithelium and mesenchyme of the first branchial arch. *Development* **127**, 217-224.

Verzi, M. P., Agarwal, P., Brown, C., McCulley, D. J., Schwarz, J. J. and Black, B. L. (2007). The transcription factor MEF2C is required for craniofacial development. *Dev Cell* **12**, 645-652.